Magnetic pulse forming of smalls aeronautic pieces

C. Sow[1], G. Bazin[2], D. Daniel[3], E. Bon[4], D. Priem[4], G. Racineux[4*]

[1] IRT Jules Verne, Chemin du Chaffault, 44340 Bouguenais, FRANCE
[2] STELIA Aerospace, 13 Boulevard des Apprentis, 44600 Saint-Nazaire, FRANCE
[3] Constellium Technology Center, CS10027 - Voreppe 38341 cedex - FRANCE
[4] Institut de Recherche en Génie Civil et Mécanique, Ecole Centrale de Nantes, 1 rue de la Noë, 44321 Nantes cedex3, FRANCE
*Corresponding author. Email: guillaume.racineux@ec-nantes.fr

Abstract

Stelia Aerospace is specialized in the forming of small (Lmax < 200 mm), medium (200 mm < Lmax < 1000 mm) and large (Lmin > 1000 mm) sheets for the aerospace industry. In order to diversify the production facilities of Stelia Aerospace we evaluated the capacity of the magnetic pulse forming to produce small parts. The material used is the aluminum alloy 2024-T4. The sheets used have a thickness of 1 mm, 2 mm and 1.6 mm. There are more than 100 references of small parts but they are all made up of a limited set of elementary geometries. These elementary geometries include: straight and interrupted straight fallen edges, convex and concave fallen edges, fallen edges holes and joggling. For each of these geometries we designed a specific inductor and die, we measured the geometric dispersions and checked the material health of the parts. At the same time, in order to facilitate tool design, we developed a numerical model in the LS DYNA computing environment. The dynamic behavior of the material was measured by dynamic compression tests on Hopkinson bar. The model was validated from the tests.

Keywords

Magnetic pulse forming, 2024-T4

1 Introduction

If an electrically conductive material is placed in a variable magnetic field $\vec{H}$ then, induced currents $\vec{j}$ appear in this piece according to the Maxwell-Faraday equation:

$$\vec{\nabla} \times \vec{E} = -\frac{\partial \vec{B}}{\partial t} \quad \text{with} \quad \vec{j} = \gamma \vec{E} \quad \text{and} \quad \vec{B} = \mu \vec{H} \tag{1}$$

where $\vec{B}$ is the magnetic induction, $\vec{E}$ the electric field, γ and μ respectively the electrical conductivity and the magnetic permeability of the material. The induced currents in the piece, being themselves subjected to the external magnetic field, they are the support of Lorentz volume forces:

$$\vec{F} = \vec{j} \times \vec{B} \tag{2}$$

In magnetic stamping, these forces are used to deform sheets and to press them on dies (V. Psyk et al., 2011). A coil replaces, in this case, the punch. The magnetic forming process has several advantages: the shaping is very short (a few microseconds), which contributes to the reduction of the cycle time in production even if the load time of the capacitors has to be considered; for some materials there is a significant gain in formability which allows, depending on the materials, to increase the limits of formability (allowing the realization of sharp edges, limiting stamping operations by reducing heat treatments, etc.); and reference is made in the literature to a limitation of the springback (V. Psyk et al., 2011).

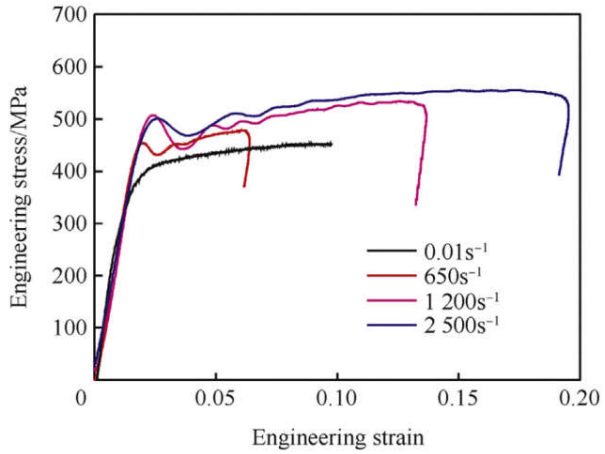

***Figure 1**: Engineering stress train curves of 2024-T4 at different strain rates (*M.Z. Xing et al. 2013*)*

For example E. Uhlmann et al. (2014) observed an increase in the formability of magnesium alloy AZ31B-O by magnetic pulse forming. M.Z. Xing et al. (2013) studied dynamic behavior of extruded 2024-T4 aluminum alloy bars at strain rates ranging from 10-2 s-1 to 2.5×10-3 s-1. Their experimental results exhibits a moderate strain hardening rate and strain rate sensitivity (**Fig. 1**). Concerning the limitation of the spring back, the experimental results which could prove it are more rare. Indeed, it is difficult to separate springback of structures dynamic effects, resulting from the impact of the sheet on the die (deformation of the die or rebound) (W. Xiong et al., 2014).

The aims of this paper is to evaluate the possibility to produce small aeronautical parts (made by Stelia Aerospace) by magnetic pulse stamping. These parts are currently manufactured by elasto-forming. The goal is to reduce cycle times while ensuring, reproducibility, satisfactory geometric and metallurgical quality of parts.

The Stelia Aerospace company manufactures several hundred references of small parts, but there are a limited number of characteristic elementary geometries of these families of parts. In this paper we present the work we have done to develop forming tools for one of these elementary geometries, the straight fallen edge. Special attention is paid to the geometric and metallurgic quality of parts. In order to evaluate dimensional reproducibility of the process, smalls series of parts were produced. Finally we present the first results obtained on a piece, called scale 1, which integrates several elementary geometries as well as simulations made in the LS DYNA computing environment.

2 Materials and methods

Fig. 2 presents different characteristic elementary geometries of parts produced by Stelia Aerospace. There are continuous (BT1) and interrupted (BT2) straight fallen edges, joggling (BT3), concave (BT4) and convex (BT5) fallen edges and fallen edges holes (BT6).

The material used is a 2024-T4 laminated aluminum alloy (**Table 1**) in 1 mm and 2 mm thick sheets manufactured by AMAG rolling GmbH with equiaxed microstructure (**Table 2**).

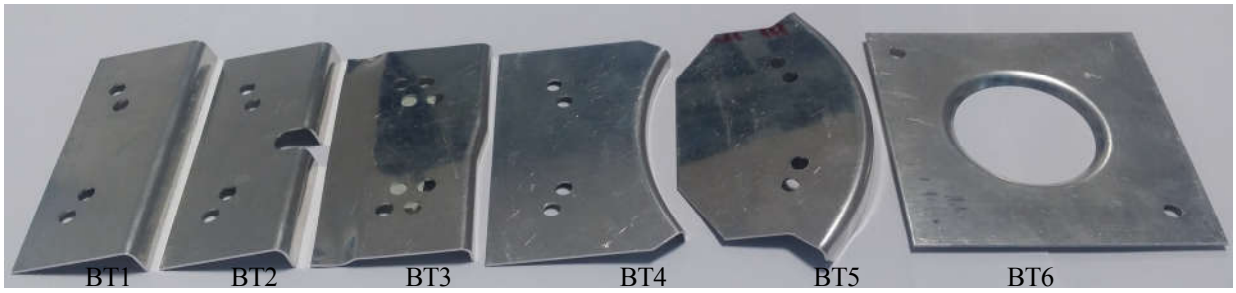

***Figure 2:**. Elementary geometries*

Alloy	Al	Si	Fe	Cu	Mn	Mg	Cr	Zn	Ti	Ga
2024-T4	98.44	0.03	0.05	4.45	0.43	1.49	0.03	0.05	0.02	0.01

***Table 1**. Chemical composition of the 2024-T4 aluminum alloy used (% by mass)*

Direction	Rm (Mpa)	Rp0,2 (Mpa)	A50 (%)
L	445	325	18
LT	435	300	18

***Table 2.** Quasi-static mechanical properties of the 2024-T4 used*

Charge voltage (kV)	Capacity (µF)	Inductance (µH)	Resistance (mΩ)	I_{max} (kA)
15	408	0.1	14	500

***Table 3.** Technical characteristics of ECN 46 kJ generator*

For this work we used a 46 kJ pulsed current generator developed at Ecole Centrale de Nantes (**Table 3**) and U-shaped coil whose active area is linear with a rectangular section (**Fig. 3** (a) and (b)). Fig. 3 (c) schematically presents the shape of magnetic field lines and currents induced in a sheet placed in front of this coil. According to equation (2), the inductor exerts a force on the sheet in the direction $\vec{z}$:

$$F = j_x B_y - j_y B_x \tag{3}$$

In order to optimize the mechanical resistance of the inductors, we have chosen to manufacture it in 110 kg steel. The dies is made of aluminum 7075.

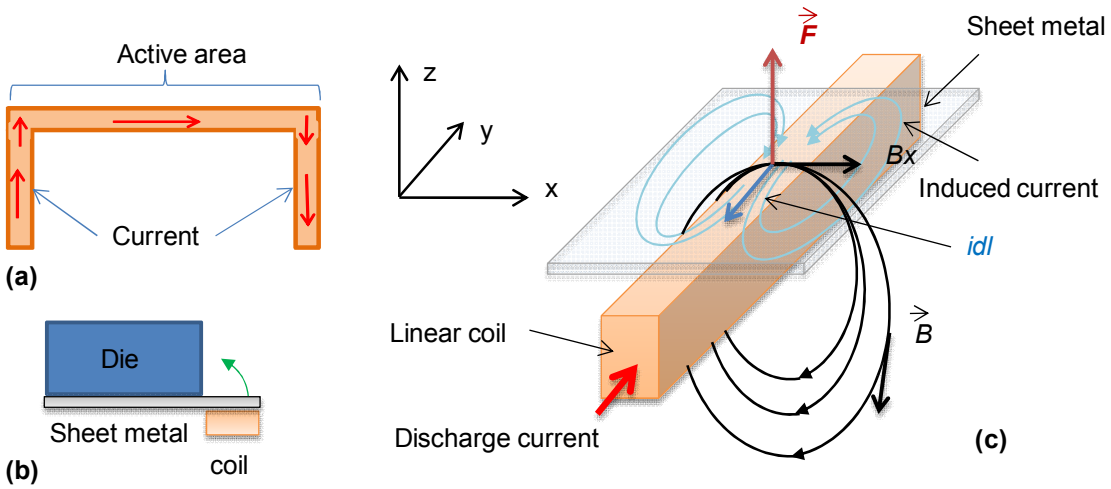

***Figure 3.** (a) Geometry of the coil, (b) Action of the coil, (c) Schematic representation of induced currents and magnetic field lines (E. Uhlmann et al., 2014)*

3 RESULTS and discussion

3.1 Forming of straight fallen edges (BT1 and BT2)

Fig. 4 presents a sequence of images captured with high speed Photron SA1 camera at 52000 i/s, in top view, for forming straight edges (BT1) with $e = 1$ mm thick sheets. The height of the edge is $H = 10$ mm and the bending inner radius is equal to $R_i = 2.5$ mm. Several observations can be made:

- It is found that the sides of the fallen edge are late compared to the center. This means that there are not enough forces applied on the sides of the sheet. This can be qualitatively explained according to the Fig. 3 (c), the straight inductor does not allow to induce currents in the sides of the sheet which induces a lack of force;
- The central part of the edge first impacts the die (image 5) and then separates from the die (image 7) before the sides impact the die in turn (image 9) and separates in turn. The separation of the sheet from the die is due to the return of waves in the sheet (rebound) which is continuous as the sheet impacts the die;
- Finally a piece is obtained with flatness, straightness and perpendicularity significant defects (image 10).

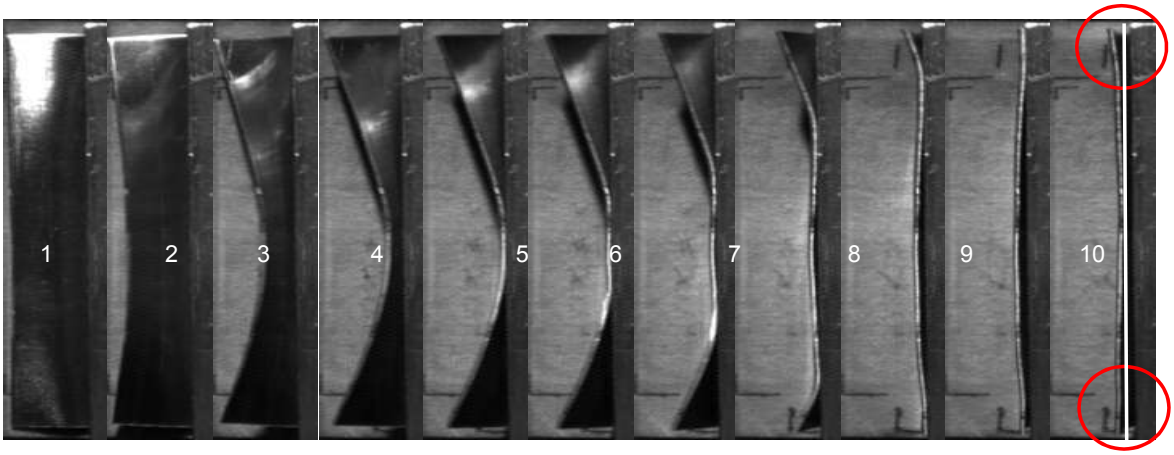

Figure 4. *BT1 forming evolution (top view)*

In addition, the analysis of the images of the film made in side view (**Fig. 5**) allowed us to measure the impact velocity of the top of the fallen edge. It is around $V = 180$ m/s. This means that on the outer part of the bending radius, assuming the existence of a neutral fiber at half the thickness of the sheet, the shear rate is about: 3×10^3 s^{-1}.

$$\dot{\varepsilon} = \frac{2\pi(R_i + e)/4 - 2\pi(R_i + e/2)/4}{2\pi(R_i + e/2)/4} \times \frac{V}{2\pi H/4} = \frac{e}{(R_i + e/2)} \times \frac{V}{\pi H} \simeq 2\times10^3 \text{ s}^{-1}.$$

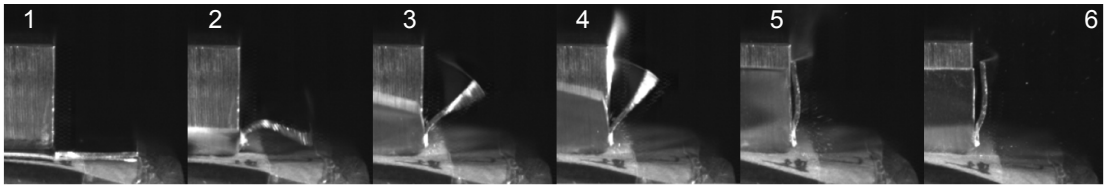

Figure 5.*BT1 forming (side view)*

To manufacture BT1 and BT2 it is therefore necessary to modified the coils at its ends in order to induce currents in the side and thus allow an uniform distribution of forces along the length of the edge. Since the rebound phenomenon cannot be avoided, it is necessary to correct the angle of the dies. By means of re-design of the coils and dies, it has been possible to manufacture corrects edges BT1 and BT2 in thickness 1 mm and 2 mm (**Fig. 6**).

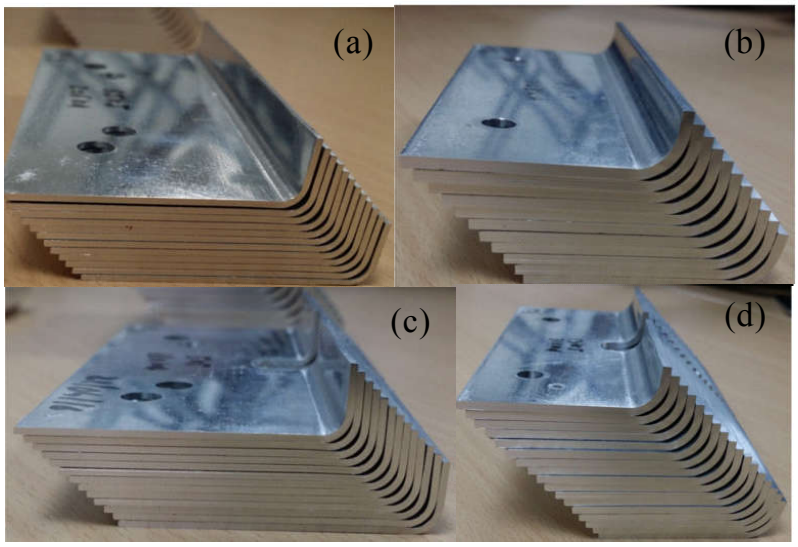

Figure 6. *(a) BT1-1 thickness 1 mm, (b) BT1-2 thickness 2 mm, (c) BT2-1 thickness 1 mm, (d) BT2-2 thickness 2 mm*

3.2 Results analysis

To evaluate the reproducibility of the process we did small series of tens pieces. Each piece was geometrically control with three-dimensional measuring machine. **Table 4** presents results of this measurement for straightness, flatness, bending radius and bending angle of straight fallen edge. The results obtained are satisfactory with regard to the tolerances imposed.

Metallurgical analysis of bending zone, after dynamic strain, do not exhibit damage of material. Coating is not affected (**Fig. 7**).

	Straightness (mm)		Flatness (mm)		Radius (mm)		Angle (°)	
	Average	Standard deviation	Average	Standard deviation	Average	Standard deviation	Average	Standard deviation
BT1-1	0.2527	0.009	0.1566	0.009	2.9117	0.097	89.8844	0.408
BT1-2	0.1177	0.018	-	-	6.3416	0.016	89.9862	0.376
BT2-1	0.146	0.02	0.118	0.014	2.782	0.011	90.608	0.577
BT2-2	0.132	0.004	-	-	6.42	0.006	91.558	0.303

Table 4. *Result of metrological control of series of ten pieces (straightness, flatness, bending radius and bending angle)*

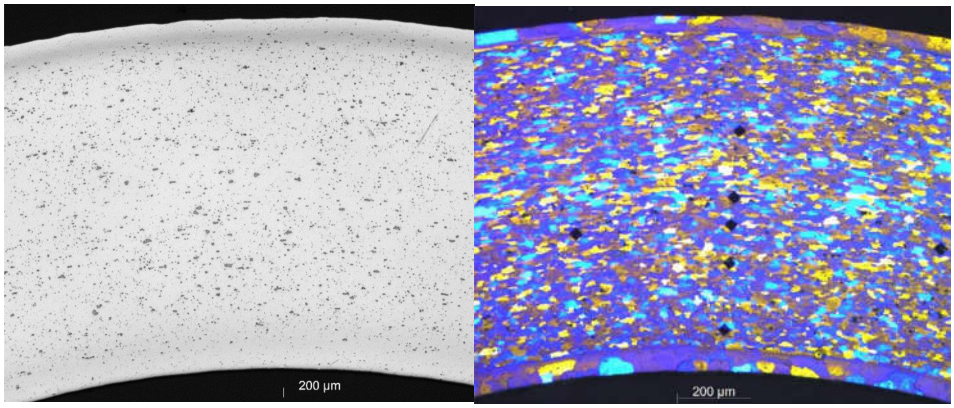

Figure 7. *Metallurgical analysis after dynamic strain (rough polishing on left, after anodic oxidation on right)*

3.3 Forming of a complex piece

Fig. 8 presents a complex piece, named "scale 1", of thickness 1.6 mm, that includes two straight fallen edges, one joggling and one hole fallen edge. According to the result of preliminary study on the design of coils to produce by magnetic pulse stamping elementary geometries, we design a coil to stamp, in one step, these four fallen edges.

The piece and coils have been modeled as solid and meshed with HEXA8 elements and the dies has been modeled as shells and meshed with QUAD4 elements. We used five elements in the thickness of the piece. The complete model contents 48000 elements.
The dies and the coil have been modeled as rigid. The modeling of the electric discharge is classically done via an electric circuit RLC circuit.

Nerveless, electromagnetic interaction between different parts of the coil require an optimization of his geometry. On the Fig. 8 one can observe that the long straight fallen edge is not correct in regards to straightness and flatness. Likewise, the joggling is not completely formed.

In order to optimize the scale 1 coil geometry, we currently doing numerical plan of experiment with LS DYNA computing environment. The numerical problem is a thermal, mechanical and electromagnetic couple problem (P. L'Eplattenier et al, 2009). The

Johnson-Cook behavior law was identified with compression dynamic test on Hopkinson bar.

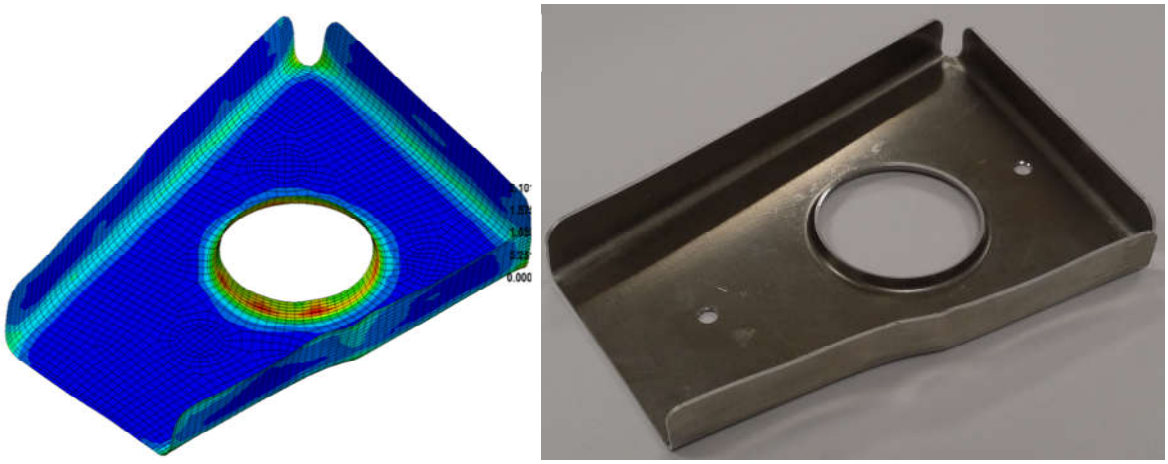

Figure 8. *Magnetic stamping of scale 1 piece (LSDyna simulation, stamped specimen*

4 Conclusion

The aim of this study was to evaluate the capacity of magnetic pulsed stamping to produce smalls aeronautical pieces made of 2024-T4 aluminum. If the coil induces homogeneous forces on full length of the fallen edge, it is possible to produce reproducibly, geometrically corrects pieces. Metallurgical analysis do not exhibit damage of 2024-T4 aluminum used. For multiple fallen edges pieces, it is necessary to optimized different parts of the coil compared to the design of coil defined for a single fallen edge. This is due to electromagnetic interaction between different part of the coil and the sheet.

5 Acknowledgement

This study is part of the HPP project managed by IRT Jules Verne (French Institute in Research and Technology in Advanced Manufacturing Technologies for Composite, Metallic and Hybrid Structures). The authors wish to associate the industrial and academic partners of this project; respectively AIRBUS, AIRBUS GROUP INNOVATIONS, CONSTELLIUM, EUROPE TECHNOLOGIES, STELIA AEROSPACE and ECOLE CENTRALE DE NANTES.

REFERENCES

V. Psyk, D. Risch, B. L. Kinsey, A. E. Tekkaya, M. Kleiner, 2011. *Electromagnetic forming-A review*. Journal of Materials Processing Technology, Volume 211, no. 5, pp. 787-829.

E. Uhlmann, L. Prasol, R.Kawalla, et al., 2014. *Extension of formability of the magnesium wrought alloy AZ31B-O at room temperature by pulse magnetic forming*. 6th International Conference on High Speed Forming.

M.Z. Xing, Y.G. Wang, Z.X. Jiang, 2013. *Dynamic fracture behaviors of selected aluminum alloys under three-point bending*. Defence Technology, vol. 9, no 4, p. 193-200.

W. Xiong, W. Wang, M. Wan, L. Pan, 2014. *Effect of the duration of electromagnetic pulse force on the rebound suppression in V-bending experiment*, 6th International Conference on High Speed Forming.

P. L'Eplattenier, G. Cook, C. Ashcraft et al., 2009. *Introduction of an Electromagnetism Module in LS-DYNA for Coupled Mechanical-Thermal-Electromagnetic Simulations*. Steel Research International, vol. 80, no 5, p. 351-358.